Thermal properties of rung-disordered two-leg quantum spin ladders: Quantum Monte Carlo study

Ulvi Kanbur*
The Graduate School of Natural and Applied Sciences, Dokuz Eylül University, 35390 Izmir, Turkey and Department of Physics, Karabük University, 78050 Karabük, Turkey

Hamza Polat and Erol Vatansever
Department of Physics, Dokuz Eylül University, 35390 Izmir, Turkey

(Received 10 May 2020; accepted 15 September 2020; published 6 October 2020)

A two-leg quenched random bond disordered antiferromagnetic spin−1/2 Heisenberg ladder system is investigated by means of stochastic series expansion quantum Monte Carlo (QMC) method. Thermal properties of the uniform and staggered susceptibilities, the structure factor, the specific heat, and the spin gap are calculated over a large number of random realizations in a wide range of disorder strength. According to our QMC simulation results, the considered system has a special temperature point at which the specific heat takes the same value regardless of the strength of the disorder. Moreover, the uniform susceptibility is shown to display the same character except for a small difference in the location of the special point. Finally, the spin gap values are found to decrease with increasing disorder parameter and the smallest gap value found in this study is well above the weak coupling limit of the clean case.

DOI: 10.1103/PhysRevE.102.042104

I. INTRODUCTION

The effect of quenched randomness on zero- and finite-temperature properties of the different types of statistical model systems is one of the fundamental problems in condensed-matter physics. The spin-1/2 Heisenberg spin chains with disorder [1,2], the spin-1/2 J-Q model on a two-dimensional (2D) square lattice [3], and quantum spin chains with power-law long-range antiferromagnetic (AFM) couplings [4] are some of the recent model systems including quenched randomness. Low-dimensional spin systems have also been an attractive topic of research thanks to the development of theoretical, experimental, and computational methods [5–13]. Besides, most of the unique properties of high-T_C superconductivity in cuprates are likely linked to the low-dimensional systems. Among the low-dimensional systems, quantum spin systems with AFM interactions show rich physical properties even in one dimension. For example, Haldane's conjecture states that AFM spin chains with integer spins exhibit a gapped spectrum, which has been supported by theoretical [14], experimental [15], and numerical (QMC) [16] studies. Also, the spin-1/2 Heisenberg coupled chains with an even number of legs have a finite spin gap (Δ) to the lowest triplet excitation. Some ladder systems have an exponentially decaying the spin-spin correlation function and the uniform susceptibility, and this can be regarded as existence of a spin gap [17]. The spin gap can be extracted from the uniform susceptibility [$\chi_u(T)$], which has the following form for the temperature regime $T \ll \Delta$ [18–20]:

$$\chi_u(T) \sim T^{-1/2} e^{-\Delta/T}. \quad (1)$$

The width of the spin gap for a two-leg ladder spin system with the isotropic coupling constant J can be roughly estimated as $\Delta \approx 0.5J$ by using QMC techniques within a reasonable computational time on modern computers [21]. The value of the spin gap can be altered or even eliminated by including disorder in the spin-spin coupling [22], choosing a different kind of a lattice topology [23,24] or applying external magnetic fields [25]. It has been shown that the spin gap is drastically reduced by a light doping on the pure system with nonmagnetic impurities [26–28]. The alteration of the spin gap due to the external effects has been investigated by also QMC simulations [29–31]. For instance, a quantum phase transition is observed in a two-leg ladder spin system with nonmagnetic impurities [30]. It is found that the random depletion of spins introduces a random Berry phase term into the nonlinear σ model [26]. Besides, the magnetic field has some remarkable effects on the physical behavior of spin ladder systems [25,32–34].

Various properties of a wide range of different ladder models have been studied, such as spin ladder systems with dimerization [35–41], zigzag ladders [23,42–45], mixed ladders [46–50]. A gapless phase has been found in two-leg zigzag ladders with frustration by benefiting from exact diagonalization and density matrix renormalization group (DMRG) methods [23]. A ferrimagnetic spin-1 and spin-1/2 mixed spin ladder has been analyzed by using spin-wave theory and bosonization techniques [48]. Thermal and ground-state properties of the similar ladder systems have been also studied by applying QMC methods [38,40,45]. The presence of quenched bond randomness may significantly affect the thermal and magnetic properties of the considered system even at low disorder concentration values. Weakly disordered anisotropic spin-1/2 ladders have been handled perturbatively

*ulvikanbur@karabuk.edu.tr

and different phases of the clean case have been detected as sensitive and insensitive to the changing disorder [51]. Furthermore, critical properties of strongly disordered systems have been mainly studied with strong disorder renormalization group method [52,53], and in combination with the DMRG method [22].

Modern QMC techniques are powerful tools to study the disordered spin ladder systems. For instance, the SSE QMC technique has been used to investigate the spin-1/2 Heisenberg quenched bond disordered ladders, and it has been found that the neighboring bond energies change sensitively with the position of the disorder in the spin-spin coupling term [54]. In Ref. [55], some unusual and interesting effects of disorder on collective excitations have been reported with the calculation of the ground-state dynamic structure factor for a ladder system with bond disorder along the legs and rungs of the ladder. To the best of our knowledge, the static properties of such a disordered model have not been investigated so far. In this paper, we investigate the thermodynamic properties of a two-leg quantum spin ladder system including a quenched bond randomness along only the rung direction. For this aim, we used the SSE QMC method with operator loop update [18,56] for varying values of the system parameters. In a nutshell, our QMC simulations show that the spin gap value tends to decrease with an increment in the disorder ratio. Moreover, a crossing point has been detected at which the disorder ratio does not play a critical role on the numerical values of both the specific heat and the uniform susceptibility curves.

The rest of the paper is planned as follows. In Sec. II, we give the details of the model and the simulation method with a common notation and formalism. The numerical results and discussion are given in Sec. III. Finally, Sec. IV contains a summary of our conclusions.

II. MODEL AND METHOD

We write the Hamiltonian of the quantum spin ladder model in a general manner to be in accord with the formulation of the SSE technique for convenience. The following Hamiltonian

$$\mathcal{H} = \sum_{b}^{N_b} J_b \boldsymbol{S_{i(b)}} \cdot \boldsymbol{S_{j(b)}} \tag{2}$$

can technically describe a wide range of models consisting of N_b bonds where a bond is a connected two sites (i and j) with coupling strength J_b. Here, $\boldsymbol{S_{i(b)}}$ are spin operators at sites $i(b)$. For the present two-leg ladder model with N sites, the bonds are all the nearest-neighbor sites with $J_b > 0$. The first N bonds are along the legs with $J_b = J$, and the remaining $N/2$ bonds are along the rung direction with $J_b = J_+$ or $J_b = J_-$ that are selected randomly from a uniform distribution with equal probabilities, and they satisfy the condition $(J_+ + J_-)/2J = 1$. An example of the quenched bond disorder on the system is shown in Fig. 1. Namely, the bonds along the rungs are drawn from the bimodal distribution

$$\mathcal{P}(J_b) = p\delta(J_b - J_+) + (1-p)\delta(J_b - J_-) \tag{3}$$

with probability $p = 1/2$.

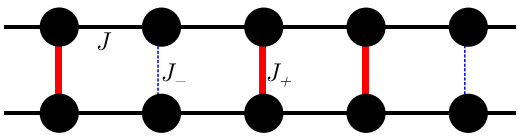

FIG. 1. An example of the quenched bond disorder configuration on a two-leg ladder system. Solid (red) and dashed (blue) lines along the rungs are the bond couplings J_+ and J_-, respectively, satisfying the condition $(J_+ + J_-)/2J = 1$. All the couplings (J) along the legs are the same.

For the $S = 1/2$ isotropic Heisenberg antiferromagnets ($J_b > 0$) within the formulation of SSE technique, the bond operator $H_b = \boldsymbol{S_{i(b)}} \cdot \boldsymbol{S_{j(b)}}$ can be divided into its diagonal and off-diagonal parts as follows:

$$H_{1,b} = \left(\tfrac{1}{4} - S^z_{i(b)} S^z_{j(b)}\right) \tag{4a}$$

$$H_{2,b} = \tfrac{1}{2}(S^+_{i(b)} S^-_{j(b)} + S^-_{i(b)} S^+_{j(b)}), \tag{4b}$$

where $H_{a,b}$ is a diagonal and off-diagonal operator for $a = 1$ and $a = 2$, respectively. The Hamiltonian can be then rewritten as follows:

$$\mathcal{H} = -\sum_{b}^{N_b} J_b (H_{1,b} - H_{2,b}) + \text{const.}, \tag{5}$$

where the constant energy term is not necessary for the implementation of the algorithm (but it should be added when calculating the energy). The nonzero matrix elements of the operators $H_{a,b}$ are all equal to $J_b/2$. Concisely, SSE QMC technique, based on the Taylor series expansion of the partition function, can be formulated as a sum of the products of the operators $H_{a,b}$ with a fixed length scheme. More details including also the implementation of the algorithm can be found in Refs. [18,56,57]. As a result, the full partition function can be given as follows:

$$\mathcal{Z} = \sum_{\alpha, S_L} (-1)^{n_2} \beta^n \frac{(L-n)!}{L!} \langle \alpha | \prod_{p=0}^{L-1} J_{b(p)} H_{a(p),b(p)} | \alpha \rangle, \tag{6}$$

where the sums are over the configurations α and all possible operator products $H_{a,b}$ including additional unit operator $H_{0,0}$ and a coupling constant $J_0 \equiv 1$, on a string of length L. Here n and n_2 are the number of nonunit and off-diagonal operators on the string, respectively. β is the inverse temperature with a unit Boltzmann constant k_B. The nonzero weights are bond dependent for an allowed configuration, and which can be written as follows:

$$W(\alpha, S_L) = \left(\frac{\beta}{2}\right)^n \frac{(L-n)!}{L!} \prod_{p=0}^{L-1} J_{b(p)}. \tag{7}$$

The numerical results are obtained for the quenched random bond two-leg ladder system of the dimension $L_x \times 2$. Here, $L_x = 256$ is the system size along the legs of the ladder. For convenience, we define a disorder strength ρ as $J_\pm = 1 \pm \rho$ where $J_+ > 1$ and $J_- < 1$ for all values of $0 \leqslant \rho \leqslant 1$. $\rho = 0.0$ corresponds to the clean case of the system.

The specific heat ($\mathcal{C}$) of the system can be easily measured by monitoring the number of nonunit operators n in the oper-

ator sequence [18],

$$\mathcal{C} = \langle n^2 \rangle - \langle n \rangle^2 - \langle n \rangle. \tag{8}$$

Static susceptibilities can be evaluated by constructing estimators from the Kubo integral [57]

$$\chi_{AB} = \int_0^\beta d\tau \langle A(\tau) B(0) \rangle, \tag{9}$$

where the integrand shows the ensemble average of an imaginary-time-dependent product with operators $A(\tau) = e^{\tau H} A(0) e^{-\tau H}$. For the case of diagonal operators A and B with eigenvalues $a(k)$ and $b(k)$, respectively, this integral can simply be written by including eigenvalues from all the propagated states [57,58],

$$\chi_{AB} = \left\langle \frac{\beta}{n(n+1)} \left[\left(\sum_{k=0}^{n-1} a(k) \right) \left(\sum_{k=0}^{n-1} b(k) \right) + \sum_{k=0}^{n-1} a(k) b(k) \right] \right\rangle. \tag{10}$$

For the conserved quantity magnetization $\mathcal{M}$, Eq. (10) reduces to the uniform susceptibility χ_u with $a(k) = b(k) = \mathcal{M}$,

$$\chi_u = \beta \langle \mathcal{M}^2 \rangle \tag{11}$$

and for the quantity staggered magnetization $\mathcal{M}_s$, Eq. (10) gives the staggered susceptibility χ_s with $a(k) = b(k) = \mathcal{M}_s(k)$,

$$\chi_s = \left\langle \frac{\beta}{n(n+1)} \left[\left(\sum_{k=0}^{n-1} \mathcal{M}_s(k) \right)^2 + \sum_{k=0}^{n-1} \mathcal{M}_s^2(k) \right] \right\rangle. \tag{12}$$

The staggered structure factor can be extracted from the second part of the Eq. (12) in runtime, which can be defined as follows:

$$\mathcal{S}(\pi, \pi) = N \langle \mathcal{M}_s^2 \rangle. \tag{13}$$

For each disorder strength $\rho = 0.0, 0.1, 0.2, \ldots, 0.9, 1.0$ the relevant quantities have been calculated for temperature values up to $T/J = 2$. 1000 random realizations of the system have been generated for each disorder parameter to get a satisfactory statistics, and each average has been used as a bin, which consists of at least 5×10^5 Monte Carlo steps (MCS) after discarding 5×10^4 MCS for the data analysis. To monitor the sample-to-sample fluctuations the running averages of the uniform susceptibility and the specific heat have been calculated in the vicinity of broad maximums and crossing points. Based on this, it is possible to say that 1000 independent realizations are found to be enough for good statistics. The standard errors have been propagated with the bootstrap resampling technique for nonlinear functions. The spin gap values have been calculated by linearizing the Eq. (1) and making a least-squares fit to it at low temperatures to find the parameter Δ.

III. RESULTS AND DISCUSSION

The temperature dependencies of the calculated quantities are around the clean case ($\rho = 0.0$) for all the disorder parameters of the system. While the disorder in the spin-spin couplings does not cause a change in the physics of the results, the considered system has a special temperature point at which the specific heat take the same value regardless of the strength of the disorder. The same finding is also observed for the uniform susceptibility with a small difference in the location of the special point. A fine sweeping around these special points has been performed to validate the existence of this coincidence of the relevant curves.

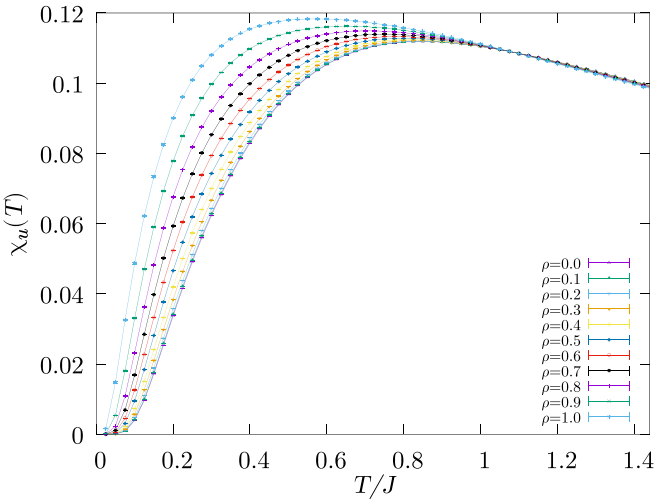

FIG. 2. Thermal variation of the uniform susceptibility for the clean case and varying values of the disorder ratios: $\rho = 0.0, 0.1, 0.2, \ldots, 0.8, 0.9$, and 1.0. The lines are added to guide the eye.

Thermal variation of the uniform susceptibility for several disorder strengths are displayed in Fig. 2. It is clear from the figure that the uniform susceptibility is nearly independent of the value of the disorder parameter at high-temperature region and a Curie behavior is present in the system. The broad maximum of the uniform susceptibility shifts to the left with a slight increment in its value as the disorder parameter takes larger values. Also, an exponentially decreasing behavior is present at low-temperature region for all disorder parameters, which indicates the existence of a spin gap.

We have calculated the crossing point for the uniform susceptibility using the intersections of the following pairs $(\rho, \rho + 0.3)$ of the disorder strengths: $(0, 0.3)$, $(0.1, 0.4)$, $(0.2, 0.5)$, $(0.3, 0.6)$, $(0.4, 0.7)$, $(0.5, 0.8)$, $(0.6, 0.9)$, and $(0.7, 1.0)$. We should also note that a number of 10^6 MCS have been used for each configuration. As shown in Fig. 3, our numerical findings suggest that the crossing temperature point is 1.083(3) for the uniform susceptibility. Using the same protocol, we have also estimated the corresponding uniform susceptibility value at the relevant crossing point to be $\chi_u^* = 0.1088(1)$. A similar point has been reported for magnetic spin susceptibilities in the spin-1/2 stacked 2-leg ladder systems [59].

As opposed to the uniform susceptibility, the maximum values of the specific heat tend to decrease with increasing value of disorder parameter as shown in the Fig. 4 and the special temperature point is more visible. Figure 5 shows the fine sweeping around the special temperature point. By benefiting from the pairs of disorder strength mentioned for the uniform susceptibility, the crossing point is estimated as

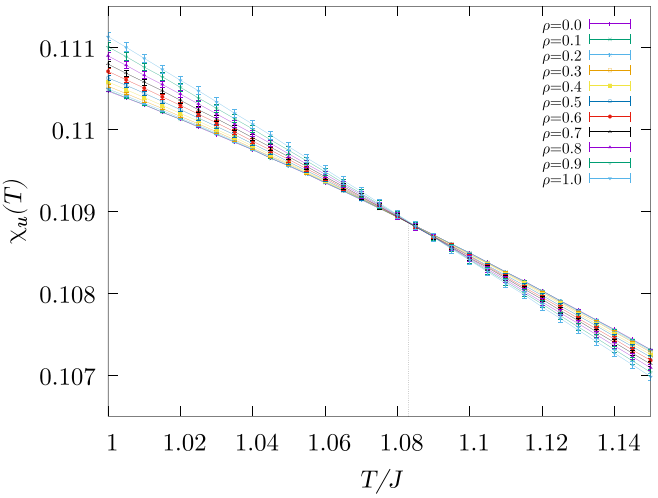

FIG. 3. Fine sweeping of the uniform susceptibility near the crossing point. The vertical dashed line corresponds to the calculated value of crossing point of the uniform susceptibility: 1.083. The lines are added to guide the eye.

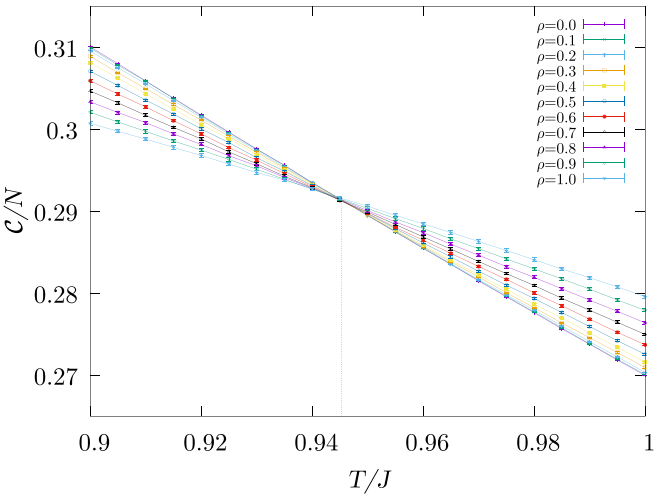

FIG. 5. Fine sweeping of the specific heat curves in the vicinity of the crossing point. The vertical dashed line corresponds to the calculated value of crossing point of the specific heat: 0.9453. The lines are added to guide the eye.

0.9453(3) with a corresponding specific heat value of $\mathcal{C}^* = 0.2912(7)$. These special points, for the specific heat and the uniform susceptibility, suggest that the point where all curves intersect can show a small difference depending on the quantity to be measured. Simulations with different system sizes up to $L_x = 512$ have shown that the crossing points are almost size independent, which leads to negligible variations in their values. Based on this finding, it is possible to say that there are two distinct crossing points in the system. Crossing points for the specific heat have been reported in various systems experimentally [60,61] and numerically [62]. The special point is found to be independent of the parameters such as pressure, magnetic field, and the local interaction of the Hubbard model. A theoretical origin of the special point has been investigated for lattice models and continuum systems [60] and the numerical results have been given for the half-filled Hubbard model in all dimensions [61]. According to these studies, the specific heat values are nearly the same despite the corresponding crossing temperatures are different from each other for all dimensions. A nearly universal crossing value of the specific heat is obtained as $\approx 0.34/k_B$, which is a little bit higher than that obtained for the rung disordered Heisenberg ladder model considered here, i.e., $\approx 0.29/k_B$. As in the case of Ref. [60], it should be noted that the rate of change of specific heat values with respect to the disorder parameter changes its sign at the crossing point to make the total entropy change to zero for the present system. Furthermore, the crossing point of the specific heat can be considered as an inflection point.

For even-leg ladders, the structure factor has a peak at a temperature that is below the relevant spin gap [63]. As it is shown in Fig. 6 for this system the peaks shift to

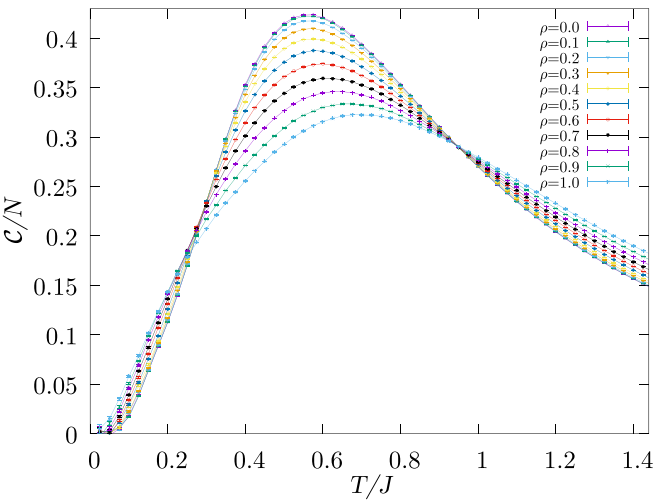

FIG. 4. Thermal variation of the specific heat curve for the clean case and all disorder ratios: $\rho = 0.0, 0.1, 0.2, \ldots, 0.8, 0.9$, and 1.0. The lines are added to guide the eye.

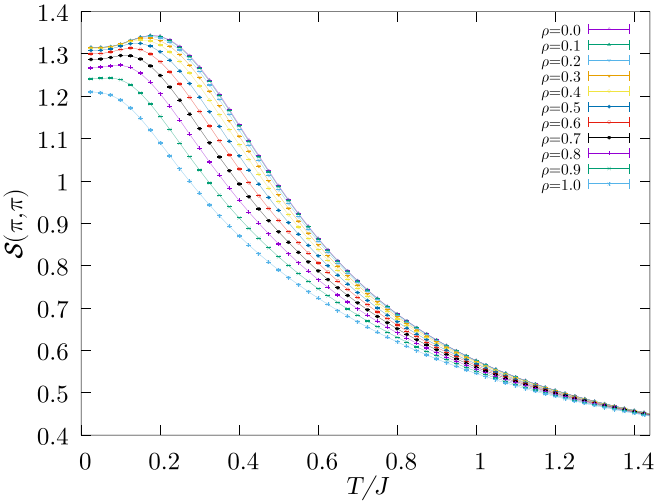

FIG. 6. Thermal variation of the structure factor for the clean case and varying values of disorder ratios: $\rho = 0.0, 0.1, 0.2, \ldots, 0.8, 0.9$, and 1.0. The lines are added to guide the eye.

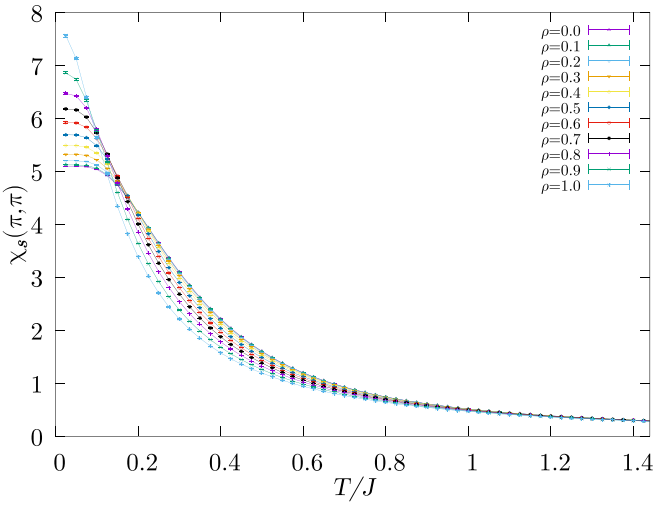

FIG. 7. Thermal variation of the staggered susceptibility for the clean case and all considered disorder strengths: $\rho = 0.0, 0.1, 0.2, \ldots, 0.8, 0.9$, and 1.0. The lines are added to guide the eye.

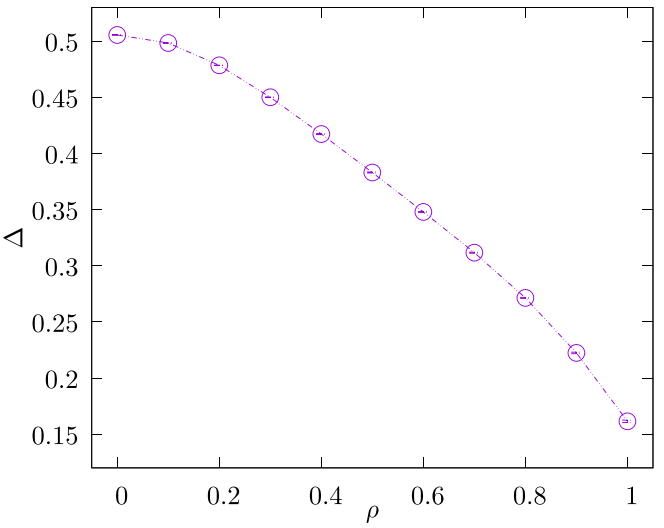

FIG. 9. The disorder ratio dependence of the spin gap value. The lines are added to guide the eye.

lower-temperature region and decrease with an increment in disorder parameter. This shows the evidence of a decreasing spin gap with increasing disorder parameter value and this observation is also confirmed by calculating the value of the spin gap using Eq. (1). For high-temperature values, the numerical results seem to be independent of the disorder parameter strength. On the other side, no crossing point is monitored in the temperature interval considered in the present study.

The staggered susceptibility has a finite value at zero temperature for all disorder parameters as can be seen from Fig. 7. It also means that adding quenched disorder does not affect the ground-state property of the system, which is known to be close to the rung-dimer state in the clean case [64]. Our QMC simulation results show that the obtained results are almost independent of the disorder parameter value at higher-temperature region and no crossing point emerges for the staggered susceptibility.

As depicted in Fig. 8, calculated spin gap values of the system are below the spin gap value of the clean case for all disorder parameters. It is also found that the spin gap values decrease with increasing disorder strength, leading an increment in the slopes of the relevant lines. For the limiting disorder parameter $\rho = 1.0$, the spin gap is around $\Delta/J \approx 0.16$, which is well above the weak coupling limit [63]. The value of the spin gap does not noticeably deviate from the clean case for $\rho = 0.1$. As a final investigation, the variation of the spin gap with disorder coupling ratio is given in Fig. 9. The decrement in the spin gap is nearly linear with the disorder parameter in the intermediate region. In particular, the spin gap declines slowly near the clean case and rapidly near to the fully disordered case.

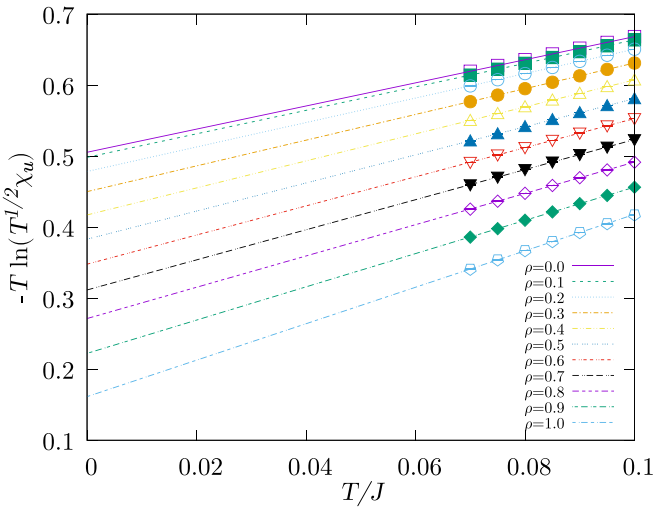

FIG. 8. Spin gap fit lines for the clean case and all disorder ratios: $\rho = 0.0, 0.1, 0.2, \ldots, 0.8, 0.9$, and 1.0. The data point at $T/J = 0.1$ for $\rho = 1.0$ has been excluded from the fitting.

IV. CONCLUSIONS

In the present paper, we used the SSE QMC technique to study the thermodynamic properties of a two-leg ladder system with the quenched random bond disorder only among the rungs of the ladder. Our simulation results show that there is a special point character in the system where the numerical results are independent of the disorder strengths for the specific heat and the uniform susceptibility, separately. The numerical values of these special points may be considered as a (nearly) universal value for the spin ladder systems. The numerical outcomes reported here also show that the averages of the disordered configurations do not tend to exhibit so different properties from the pure part. This may be a result of the bond randomness including the same kind of interactions, which is introduced only in the rung direction of the ladder system. Another important result emerging in this study is that the spin gap values are found to decrease with increasing disorder parameter, as in the case of decreasing rung coupling values in the clean system. Finally, it would be interesting to study

systems with disorder along only the leg or in both directions, as the disorder effects may exhibit interesting physical properties. Such kind of study may be the subject of future work. On the theoretical side, the equivalence of the half-filled Hubbard and the Heisenberg models might lead to exact expressions to extract crossing points.

ACKNOWLEDGMENTS

The authors would like to thank S. Wessel for many useful comments and discussion on the manuscript. The numerical calculations reported in this paper were performed at TÜBİTAK ULAKBİM (Turkish agency), High Performance and Grid Computing Center (TRUBA Resources).

[1] Y.-R. Shu, D.-X. Yao, C.-W. Ke, Y.-C. Lin, and A. W. Sandvik, Properties of the random-singlet phase: From the disordered Heisenberg chain to an amorphous valence-bond solid, Phys. Rev. B **94**, 174442 (2016).

[2] T. Shiroka, F. Eggenschwiler, H.-R. Ott, and J. Mesot, From order to randomness: Onset and evolution of the random-singlet state in bond-disordered $BaCu_2(Si_{1-x}Ge_x)_2O_7$ spin-chain compounds, Phys. Rev. B **99**, 035116 (2019).

[3] L. Liu, H. Shao, Y.-C. Lin, W. Guo, and A. W. Sandvik, Random-Singlet Phase in Disordered Two-Dimensional Quantum Magnets, Phys. Rev. X **8**, 041040 (2018).

[4] N. Moure, H.-Y. Lee, S. Haas, R. N. Bhatt, and S. Kettemann, Disordered quantum spin chains with long-range antiferromagnetic interactions, Phys. Rev. B **97**, 014206 (2018).

[5] J. Akimitsu, Towards higher-T_c superconductors, Proc. Jpn. Acad. Ser. B **95**, 321 (2019).

[6] E. J. König, A. M. Tsvelik, and P. Coleman, Renormalization group analysis for the quasi-1d superconductor $BaFe_2S_3$, Phys. Rev. B **98**, 184517 (2018).

[7] N. D. Patel, A. Nocera, G. Alvarez, R. Arita, A. Moreo, and E. Dagotto, Magnetic properties and pairing tendencies of the iron-based superconducting ladder $BaFe_2S_3$: Combined *ab initio* and density matrix renormalization group study, Phys. Rev. B **94**, 075119 (2016).

[8] M.-T. Suzuki, R. Arita, and H. Ikeda, First-principles study of magnetic properties in Fe-ladder compound $BaFe_2S_3$, Phys. Rev. B **92**, 085116 (2015).

[9] J. Yu, M. Wang, B. A. Frandsen, H. Sun, J. Yin, Z. Liu, S. Wu, M. Yi, Z. Xu, A. Acharya, Q. Huang, E. Bourret-Courchesne, J. W. Lynn, and R. J. Birgeneau, Structural, magnetic, and electronic evolution of the spin-ladder system $BaFe_2S_{3-x}Se_x$ with isoelectronic substitution, Phys. Rev. B **101**, 235134 (2020).

[10] Y. Zhang, L.-F. Lin, A. Moreo, S. Dong, and E. Dagotto, Magnetic states of iron-based two-leg ladder tellurides, Phys. Rev. B **100**, 184419 (2019).

[11] Y. Zhang, L. Lin, J.-J. Zhang, E. Dagotto, and S. Dong, Pressure-driven phase transition from antiferromagnetic semiconductor to nonmagnetic metal in the two-leg ladders AFe_2X_3(A = Ba or K, X = S or Se), Phys. Rev. B **95**, 115154 (2017).

[12] Y. Zhang, L.-F. Lin, J.-J. Zhang, E. Dagotto, and S. Dong, Sequential structural and antiferromagnetic transitions in $BaFe_2S_3$ under pressure, Phys. Rev. B **97**, 045119 (2018).

[13] A. Vasiliev, O. Volkova, E. Zvereva, and M. Markina, Milestones of low-D quantum magnetism, npj Quantum Mater. **3**, 18 (2018).

[14] I. Affleck and E. H. Lieb, A proof of part of Haldane's conjecture on spin chains, Lett. Math. Phys. **12**, 57 (1986).

[15] W. J. L. Buyers, R. M. Morra, R. L. Armstrong, M. J. Hogan, P. Gerlach, and a. K. Hirakawa, Experimental Evidence for the Haldane Gap in a Spin-1 Nearly Isotropic, Antiferromagnetic Chain, Phys. Rev. Lett. **56**, 371 (1986).

[16] M. P. Nightingale and H. W. J. Blöte, Gap of the linear spin-1 Heisenberg antiferromagnet: A Monte Carlo calculation, Phys. Rev. B **33**, 659 (1986).

[17] E. Dagotto and T. M. Rice, Surprises on the way from one- to two-dimensional quantum magnets: The ladder materials, Science **271**, 618 (1996).

[18] A. W. Sandvik, Computational studies of quantum spin systems, AIP Conf. Proc. **1297**, 135 (2010).

[19] B. Frischmuth, B. Ammon, and M. Troyer, Susceptibility and low-temperature thermodynamics of spin-1/2 Heisenberg ladders, Phys. Rev. B **54**, R3714 (1996).

[20] S. R. White, Equivalence of the antiferromagnetic Heisenberg ladder to a single S=1 chain, Phys. Rev. B **53**, 52 (1996).

[21] T. Barnes, E. Dagotto, J. Riera, and E. S. Swanson, Excitation spectrum of Heisenberg spin ladders, Phys. Rev. B **47**, 3196 (1993).

[22] R. Mélin, Y.-C. Lin, P. Lajkó, H. Rieger, and F. Iglói, Strongly disordered spin ladders, Phys. Rev. B **65**, 104415 (2002).

[23] D. Maiti, D. Dey, and M. Kumar, Frustrated spin-1/2 ladder with ferro- and antiferromagnetic legs, J. Magn. Magn. Mater. **446**, 170 (2018).

[24] A. Metavitsiadis and S. Eggert, Competing phases in spin ladders with ring exchange and frustration, Phys. Rev. B **95**, 144415 (2017).

[25] R. Chitra and T. Giamarchi, Critical properties of gapped spin-chains and ladders in a magnetic field, Phys. Rev. B **55**, 5816 (1997).

[26] N. Nagaosa, A. Furusaki, M. Sigrist, and H. Fukuyama, Nonmagnetic impurities in spin gap systems, J. Phys. Soc. Jpn. **65**, 3724 (1996).

[27] I. Y. Korenblit, Lightly doped spin ladders at low temperatures, Phys. Rev. B **56**, 5057 (1997).

[28] H.-J. Mikeska, U. Neugebauer, and U. Schollwöck, Spin ladders with nonmagnetic impurities, Phys. Rev. B **55**, 2955 (1997).

[29] Y. Iino and M. Imada, Effects of nonmagnetic impurity doping on spin ladder system, J. Phys. Soc. Jpn. **65**, 3728 (1996).

[30] Y. Motome, N. Katoh, N. Furukawa, and M. Imada, Impurity effect on spin ladder system, J. Phys. Soc. Jpn. **65**, 1949 (1996).

[31] A. Lavarélo, G. Roux, and N. Laflorencie, Magnetic responses of randomly depleted spin ladders, Phys. Rev. B **88**, 134420 (2013).

[32] T. Giamarchi and A. M. Tsvelik, Coupled ladders in a magnetic field, Phys. Rev. B **59**, 11398 (1999).

[33] C. Rüegg, K. Kiefer, B. Thielemann, D. F. McMorrow, V. Zapf, B. Normand, M. B. Zvonarev, P. Bouillot, C. Kollath, T. Giamarchi, S. Capponi, D. Poilblanc, D. Biner, and K. W. Krämer, Thermodynamics of the Spin Luttinger Liquid in

a Model Ladder Material, Phys. Rev. Lett. **101**, 247202 (2008).
[34] S. Wessel, M. Olshanii, and S. Haas, Field-Induced Magnetic Order in Quantum Spin Liquids, Phys. Rev. Lett. **87**, 206407 (2001).
[35] D. C. Cabra and M. D. Grynberg, Magnetization plateaus in dimerized spin-ladder arrays, Phys. Rev. B **62**, 337 (2000).
[36] G. I. Japaridze and S. Mahdavifar, Magnetic phase diagram of the dimerized spin S = 1/2 ladder, Eur. Phys. J. B **68**, 59 (2009).
[37] J. Chen, K.-L. Yao, and L.-J. Ding, Identification of intrinsic gapped behavior in spin-1/2 ladder with staggered dimerization, Physica A **391**, 2306 (2012).
[38] Q.-H. Chen, L.-F. Guo, and P. Li, The ground state phase diagrams and low-energy excitation of dimer XXZ spin ladder, Physica E **64**, 188 (2014).
[39] T. Kariyado and Y. Hatsugai, Topological order parameters of the spin-$\frac{1}{2}$ dimerized Heisenberg ladder in magnetic field, Phys. Rev. B **91**, 214410 (2015).
[40] J. Jahangiri, F. Amiri, and S. Mahdavifar, Thermodynamic behavior near the quantum orders in dimerized spin S=1/2 two-leg ladders, J. Magn. Magn. Mater. **439**, 22 (2017).
[41] M. Shahri Naseri and S. Mahdavifar, The magnetic properties of spin-1/2 two-leg ladders with dimerized legs and trimerized modulation of rung exchange, Physica A **474**, 107 (2017).
[42] S. Chen, H. Büttner, and J. Voit, Phase Diagram of an Asymmetric Spin Ladder, Phys. Rev. Lett. **87**, 087205 (2001).
[43] J. A. Hoyos and E. Miranda, Phase diagrams and universality classes of random antiferromagnetic spin ladders, Phys. Rev. B **69**, 214411 (2004).
[44] J. E. Bunder and H.-H. Lin, Generic short-range interactions in two-leg ladders, Phys. Rev. B **79**, 045132 (2009).
[45] I. L. Danilovich, E. V. Karpova, I. V. Morozov, A. V. Ushakov, S. V. Streltsov, A. A. Shakin, O. S. Volkova, E. A. Zvereva, and A. N. Vasiliev, Spin-singlet quantum ground state in zigzag spin ladder $Cu(CF3COO)_2$, ChemPhysChem **18**, 2482 (2017).
[46] A. Kolezhuk and H.-J. Mikeska, Mixed spin ladders with exotic ground states, Eur. Phys. J. B **5**, 543 (1998).
[47] M. T. Batchelor, J. de Gier, and M. Maslen, Exactly solvable su(N) mixed spin ladders, J. Stat. Phys. **102**, 559 (2001).
[48] D. N. Aristov and M. N. Kiselev, Ferrimagnetic mixed-spin ladders in weak- and strong-coupling limits, Phys. Rev. B **70**, 224402 (2004).
[49] M. T. Batchelor, X.-W. Guan, N. Oelkers, and Z.-J. Ying, Quantum phase diagram of an exactly solved mixed spin ladder, J. Stat. Phys. **116**, 571 (2004).
[50] H. A. Zad and N. Ananikian, Phase transitions and magnetization of the mixed-spin Ising–Heisenberg double sawtooth frustrated ladder, J. Phys.: Condens. Matter **30**, 165403 (2018).
[51] E. Orignac and T. Giamarchi, Weakly disordered spin ladders, Phys. Rev. B **57**, 5812 (1998).
[52] F. Iglói and C. Monthus, Strong disorder RG approach of random systems, Phys. Rep. **412**, 277 (2005).
[53] T. Vojta, Phases and phase transitions in disordered quantum systems, AIP Conf. Proc. **1550**, 188 (2013).
[54] K. Trinh and S. Haas, Bond disorder in even-leg Heisenberg ladders, Phys. Rev. B **87**, 075137 (2013).
[55] M. Hörmann, P. Wunderlich, and K. P. Schmidt, Dynamic Structure Factor of Disordered Quantum Spin Ladders, Phys. Rev. Lett. **121**, 167201 (2018).
[56] A. W. Sandvik, Stochastic series expansion method with operator-loop update, Phys. Rev. B **59**, R14157 (1999).
[57] A. W. Sandvik, A generalization of Handscomb's quantum Monte Carlo scheme-application to the 1D Hubbard model, J. Phys. A: Math. Gen. **25**, 3667 (1992).
[58] A. W. Sandvik, Finite-size scaling of the ground-state parameters of the two-dimensional Heisenberg model, Phys. Rev. B **56**, 11678 (1997).
[59] D. C. Johnston, M. Troyer, S. Miyahara, D. Lidsky, K. Ueda, M. Azuma, Z. Hiroi, M. Takano, M. Isobe, Y. Ueda, M. A. Korotin, V. I. Anisimov, A. V. Mahajan, and L. L. Miller, arXiv:cond-mat/0001147 [cond-mat.str-el].
[60] D. Vollhardt, Characteristic Crossing Points in Specific Heat Curves of Correlated Systems, Phys. Rev. Lett. **78**, 1307 (1997).
[61] N. Chandra, M. Kollar, and D. Vollhardt, Nearly universal crossing point of the specific heat curves of Hubbard models, Phys. Rev. B **59**, 10541 (1999).
[62] A. Georges and W. Krauth, Physical properties of the half-filled Hubbard model in infinite dimensions, Phys. Rev. B **48**, 7167 (1993).
[63] M. Greven, R. J. Birgeneau, and U. J. Wiese, Monte Carlo Study of Correlations in Quantum Spin Ladders, Phys. Rev. Lett. **77**, 1865 (1996).
[64] T. Miyazaki, M. Troyer, M. Ogata, K. Ueda, and D. Yoshioka, Susceptibilities of $Sr(Cu_{1-x}Zn_x)_2O_3$ studied by quantum monte carlo simulation, J. Phys. Soc. Jpn. **66**, 2580 (1997).